Inorg. Chem. **2003**, *42*, 2301–2310

Importance of the C–H···N Weak Hydrogen Bonding on the Coordination Structures of Manganese(III) Porphyrin Complexes

Akira Ikezaki[†] **and Mikio Nakamura***[,†,‡]

Department of Chemistry, School of Medicine, Toho University, Tokyo 143-8540, Japan, and Division of Biomolecular Science, Graduate School of Science, Toho University, Funabashi 274-8510, Japan

Received October 14, 2002

The reactions between Mn(Por)Cl and $Bu_4N^+CN^-$ have been examined in various solvents by UV–vis and ^{1}H NMR spectroscopy, where Por's are dianions of *meso*-tetraisopropylporphyrin (T^{i}PrP), *meso*-tetraphenylporphyrin (TPP), *meso*-tetrakis(*p*-(trifluoromethyl)phenyl)porphyrin (*p*-CF_3-TPP), *meso*-tetramesitylporphyrin (TMP), and *meso*-tetrakis-(2,6-dichlorophenyl)porphyrin (2,6-Cl_2-TPP). Population ratios of the reaction products, Mn(Por)(CN) and $[Mn(Por)(CN)_2]^-$, have been sensitively affected by the solvents used. In the case of Mn(T^{i}PrP)Cl, the following results are obtained: (i) The bis-adduct is preferentially formed in dipolar aprotic solvents such as DMSO, DMF, and acetonitrile. (ii) Both the mono- and bis-adduct are formed in the less polar solvents such as CH_2Cl_2 and benzene though the complete conversion to the bis-adduct is achieved with much smaller amount of the ligand in benzene solution. (iii) Only the mono-adduct is formed in $CHCl_3$ solution even in the presence of a large excess of cyanide. (iv) Neither the mono- nor the bis-adduct is obtained in methanol solution. The results mentioned above have been explained in terms of the C–H···N and O–H···N hydrogen bonding in chloroform and methanol solutions, respectively, between the solvent molecules and cyanide ligand; hydrogen bonding weakens the coordination ability of cyanide and reduces the population of the bis-adduct. The importance of the C–H···N weak hydrogen bonding is most explicitly shown in the following fact: *while the starting complex is completely converted to the bis-adduct in CH_2Cl_2 solution, the conversion from the mono- to the bis-adduct is not observed even in the presence of 7000 equiv of $Bu_4N^+CN^-$ in $CHCl_3$ solution.* The effective magnetic moments of the bis-adduct has been determined by the Evans method to be 3.2 μ_B at 25 °C, suggesting that the complex adopts the usual $(d_{xy})^2(d_{xz}, d_{yz})^2$ electron configuration despite the highly ruffled porphyrin core expected for $[Mn(T^iPrP)(CN)_2]^-$. The spin densities of $[Mn(T^iPrP)(CN)_2]^-$ centered on the π MO have been determined on the basis of the ^{1}H and ^{13}C NMR chemical shifts. Estimated spin densities are as follows: *meso*-carbon, –0.0014; α-pyrrole carbon, –0.0011; β-pyrrole carbon, +0.0066; pyrrole nitrogen, –0.022. The spin densities at the pyrrole carbon and *meso* nitrogen atoms are much smaller than those of the corresponding $[Mn(TPP)(CN)_2]^-$, which is ascribed to the nonplanar porphyrin ring of $[Mn(T^iPrP)(CN)_2]^-$. This study has reveled that the C–H···N weak hydrogen bonding is playing an important role in determining the stability of the manganese(III) complexes.

Introduction

C−H···X (X = O, N, etc.) type weak hydrogen bondings together with C−H···π interaction are the focus of attention in an interdisciplinary area encompassing organic chemistry, inorganic chemistry, biochemistry, and material science, because these weak interactions sometimes play a crucial role for the determination of physicochemical properties of simple synthetic compounds as well as complicated biomolecules.[1−3] Some years ago, La Mar and co-workers pointed out that the electronic state of $[Fe(TPP)(CN)_2]^-$ is perturbed by the solvents due to the hydrogen bonding between the coordinated cyanide and solvent molecules.[4] We have

* To whom correspondence should be addressed. E-mail: mnakamu@med.toho-u.ac.jp.
[†] School of Medicine.
[‡] Graduate School of Science.

(1) Desiraju G. R.; Steiner, T. The Weak Hydrogen Bond. In *Structural Chemistry and Biology*; Oxford University Press: New York, 1999.
(2) Nishio, M.; Hirota, M.; Umezawa, Y. *The CH/π interaction, evidence, nature, and consequences*; Wiley-VCH: New York, 1998.
(3) Steiner, T. *Chem. Commun.* **1997**, 727−734.
(4) La Mar, G. N.; Gaudio, J. D.; Frye, J. S. *Biochim. Biophys. Acta* **1977**, *498*, 422−435.

10.1021/ic0206138 CCC: $25.00
Published on Web 03/01/2003

recently reported that the ground-state electron configuration of low-spin dicyano[*meso*-tetrakis(2,4,6-triethylphenyl)porphyrinato]ferrate(III), $[Fe(Et\text{-}TPP)(CN)_2]^-$, is sensitively affected by the solvents used.[5] For example, while the complex exhibits the common $(d_{xy})^2(d_{xz}, d_{yz})^3$ electron configuration in nonpolar and dipolar aprotic solvents such as benzene, toluene, DMSO, and DMF, it shows the less common $(d_{xz}, d_{yz})^4(d_{xy})^1$ electron configuration in a protic solvent such as methanol. The results have been explained in terms of the O−H···N hydrogen bonding between methanol and the coordinated cyanide ligands; the O−H···N hydrogen bonding stabilizes the cyanide p_π* orbital, which in turn stabilizes the iron d_π (d_{xz} and d_{yz}) orbitals by the strong iron (d_π)−cyanide (p_π*) interactions.[5,6] Extensive ^{1}H and ^{13}C NMR experiments together with EPR studies have revealed that even $CHCl_3$ and CH_2Cl_2 stabilize the $(d_{xz}, d_{yz})^4(d_{xy})^1$ electron configuration though the degree of stabilization is much larger in $CHCl_3$ than in CH_2Cl_2 solution. The results have been ascribed to the C−H···N weak hydrogen bonding between these solvents and the coordinated cyanide ligands.[1,5] Although few examples have been reported on the physicochemical properties showing some difference between $CHCl_3$ and CH_2Cl_2 solutions, such a difference could be a general matter in various aspects of coordination chemistry. Scheidt and co-workers reported the formation constants of the mono- and bis(cyanide) adducts in the reaction between Mn(TPP)(OH) and KCN in methanol by UV−vis spectroscopy.[7] We have expected that the population ratios of these products, [mono]/[bis], in various solvents could be a good probe to elucidate the solvent effects. In this study, we have examined the reactions between Mn(Por)Cl and $Bu_4N^+CN^-$ in various solvents such as C_6H_6, $C_6H_5CH_3$, CH_2Cl_2, $CHCl_3$, CH_3CN, DMSO, DMF, and CH_3OH, where Por stands for T^{i}PrP, TPP, and *p*-CF_3-TPP. Herein, we report that the population ratios are quite different among these solvents, even between CH_2Cl_2 and $CHCl_3$. We also report the spin distribution on the porphyrin carbon and nitrogen atoms in ruffled $[Mn(T^iPrP)(CN)_2]^-$ and compare them with those of planar $[Mn(TPP)(CN)_2]^-$ originally reported by Goff and Hansen.[8]

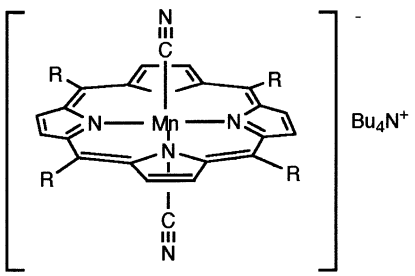

$[Mn(TRP)(CN)_2]^-Bu_4N^+$

Experimental Section

Abbreviations: T^{i}PrP, TPP, *p*-CF_3-TPP, TMP, 2,6-Cl_2-TPP, and OEP, dianions of *meso*-tetraisopropylporphyrin, *meso*-tetraphenylporphyrin, *meso*-tetrakis(*p*-(trifluoromethyl)phenyl)porphyrin, *meso*-tetramesitylporphyrin, *meso*-tetrakis(2,6-dichlorophenyl)porphyrin, and 2,3,7,8,12,13,17,18-octaethylporphyrin; Mn(T^{i}PrP)Cl, chloro(*meso*-tetraisopropylporphyrinato)manganese(III); Mn(T^{i}PrP)(CN), cyano(*meso*-tetraisopropylporphyrinato)manganese(III); $[Mn(T^iPrP)(CN)_2]^-Bu_4N^+$, tetrabutylammonium dicyano(*meso*-tetraisopropylporphyrinato)manganate(III); ^{t}BuNC, *tert*-butyl isocyanide.

Materials. $Bu_4N^+CN^-$ was purchased from Aldrich. Highly pure DMSO, DMF, methanol, ethanol, 2-propanol, and CCl_4 were purchased from Wako or Kanto. All the deuterated solvents were purchased from Merck. $CHCl_3$ and $CDCl_3$ were washed several times with concentrated sulfuric acid and then with dilute sodium carbonate solution and water.[9] They were then dried over K_2CO_3 and distilled in an argon atmosphere shortly before use. Acetonitrile, benzene, and toluene were dried and then distilled.

Synthesis. Free-base porphyrins $(TPP)H_2$, $(p\text{-}CF_3\text{-}TPP)H_2$, $(TMP)H_2$, and $(2,6\text{-}Cl_2\text{-}TPP)H_2$ were prepared according to the literatures.[10−13] Manganese(III) complexes, Mn(Por)Cl, such as Mn(TPP)Cl, Mn(*p*-CF_3-TPP)Cl, Mn(TMP)Cl, and Mn(2,6-Cl_2-TPP)Cl were prepared by reaction of porphyrins (Por's) with $MnCl_2$ in refluxing DMF solution.[14]

Synthesis of Mn(T^{i}PrP)Cl. To a 500 mL three-neck flask with a septum, reflux condenser, and argon inlet port were charged $(T^iPrP)H_2$ (201 mg, 0.410 mmol),[15,16] K_2CO_3 (568 mg), and $CHCl_3$ (300 mL). The solution was purged with argon for 15 min and was then refluxed. The methanol solution (20 mL) of $MnCl_2$ (106 mg, 0.842 mmol) was added to the refluxed solution repeatedly with the interval of 1 h. The total amount of $MnCl_2$ added was 530 mg (4.20 mmol). The solution was then rotary evaporated to dryness. The solid thus obtained was dissolved in 50 mL of CH_2Cl_2 and washed three times with 1 M HCl solution. The organic layer was washed with water and dried over anhydrous Na_2SO_4 and was then rotary evaporated to dryness. Mn(T^{i}PrP)Cl was purified by column chromatography on alumina with chloroform eluent. After rotary evaporation of the chloroform solution, a green solid product Mn(T^{i}PrP)Cl was recovered, which was vacuum-dried at 60 °C. Yield: 187 mg (77%). UV−vis (CH_2Cl_2; λ_{max}, nm (log ϵ)): 328 (4.4), 378 (4.5), 400 (4.5), 480 (4.9), 545 (3.6), 598 (3.7), 636 (4.0). ^{1}H NMR (CD_2Cl_2, 25 °C; δ, ppm): −19.4 (8H, Py-H), 9.5 (4H, CH), 3.2 (24H, CH_3). ^{13}C NMR (CD_2Cl_2, 25 °C; δ, ppm): 475 (α-Py), −153 (β-py), 216 (*meso*), 47.9 (CH), 112.5 (CH_3).

Synthesis of $[Co(T^iPrP)(CN)_2]^-Bu_4N^+$. Co(T^{i}PrP) was synthesized by the literature method.[17] A CH_2Cl_2 solution containing Co(T^{i}PrP) (50 mg, 0.091 mmol) and $Bu_4N^+CN^-$ (98 mg, 0.37 mmol) was stirred for 1 min under air. The solution was washed with water for three times. After the removal of the solvent, $[Co(T^iPrP)(CN)_2]^-Bu_4N^+$ was recrystallized from CH_2Cl_2 and

(5) Ikezaki, A.; Nakamura, M. *Inorg. Chem*. **2002**, *41*, 2761−2768.
(6) Ikezaki, A.; Ikeue, T.; Nakamura, M. *Inorg. Chim. Acta* **2002**, *335*, 91−99.
(7) Scheidt, W. R.; Lee, Y. J.; Luangdilok, W.; Haller, K. J.; Anzai, K.; Hatano, K. *Inorg. Chem*. **1983**, *22*, 1516−1522.
(8) Hansen, A. P.; Goff, H. M. *Inorg. Chem.* **1984**, *23*, 4519−4525.
(9) Riddick, J. A.; Bunger, W. B. In *Organic Solvents, Techniques of Chemistry*; Wiley-Interscience: New York, 1970; Vol. II.
(10) Adler, A. D.; Longo, F. R.; Finarelli, J. D.; Goldmacher, J.; Assour, J.; Korsakoff, L. *J. Org. Chem.* **1967**, *32*, 476.
(11) Eaton, S. S.; Eaton, G. R. *Inorg. Chem.* **1976**, *15*, 134−139.
(12) Lindsey, J. S.; Wagner, R. W. *J. Org. Chem.* **1989**, *54*, 828−836.
(13) Hill, C. L.; Williamson, M. M. *J. Chem. Soc. Chem. Commun*. **1985**, 1228−1229.
(14) Adler, A. D.; Longo, F. R.; Kampas, F.; Kim, J. *J. Inorg. Nucl. Chem.* **1970**, *32*, 2443−2445.
(15) Ema, T.; Senge, M. O.; Nelson, N. Y.; Ogoshi, H.; Smith, K. M. *Angew. Chem., Int. Ed. Engl*. **1994**, *33*, 1879−1881.
(16) Senge, M. O.; Bischoff, I.; Nelson, N. Y.; Smith, K. M. *J. Porphyrins Phthalocyanines* **1999**, *3*, 99−116.
(17) Saitoh, T.; Ikeue, T.; Ohgo, Y.; Nakamura, M. *Tetrahedron* **1997**, *53*, 12487−12496.

Table 1. UV−Vis Absorption Maxima (λ_{max}, nm) in Various Solvents

solvents	λ_{max}/nm						
			Mn(T^{i}PrP)Cl				
C_6H_6	331	373	401	481	545	600	639
$C_6H_5CH_3$	331	373	402	481	547	600	640
CH_2Cl_2	328	378	400	480	545	598	636
$CHCl_3$	327	377	401	481	546	597	637
CH_3CN	326			478	543	595	634
DMSO	325	375	411	469	538	585	625
DMF	323	378	401, 414	471	539	586	624
CH_3OH	320	377	398, 415	470	539	582	622
			Mn(T^{i}PrP)(CN)				
C_6H_6	334	385	407	494	558		656
$C_6H_5CH_3$	335	387	408	494	555		657
CH_2Cl_2	333	386	408	493	555		656
$CHCl_3$	331	387	407	494	556		653
CH_3CN	332	385	407	470, 490	550	588	651
DMSO	−	−	−	−	−	−	−
DMF	331	384	409	472, 490	547	589	654
CH_3OH	318	379	409	470	545	584	636
			[Mn(T^{i}PrP)(CN)$_2$]$^-$				
C_6H_6	339	414	440	464	551	585	711
$C_6H_5CH_3$	339	415	439	465	550	586	710
CH_2Cl_2	−	413	436	464	549	582	708
$CHCl_3$	−	−	−	−	−	−	−
CH_3CN	336	410	434	461	547	582	708
DMSO	338	414	438	465	549	584	710
DMF	338	415	438	462	548	585	708
CH_3OH	−	−	−	−	−	−	−

hexane to give 74 mg (97%) of the pure complex. UV−vis (CH_2Cl_2; λ_{max}, nm (log ϵ)): 371 (4.3), 465 (5.0), 55 4(3.2), 604 (3.7), 650 (4.1). ^{1}H NMR (CD_2Cl_2, 25 °C; δ, ppm): 9.13 (8H, Py-H), 4.80 (4H, CH), 2.14 (24H, CH_3). ^{13}C NMR (CD_2Cl_2, 25 °C; δ, ppm): 140.4 (α-Py), 131.2 (β-py), 122.3 (*meso*), 34.7 (CH), 28.9 (CH_3).

Spectral Measurements. UV−vis spectra were measured on a Shimadzu MultiSpec-1500 spectrophotometer at ambient temperature. A solution of Mn(T^{i}PrP)Cl was prepared in a graduated flask and used as a standard solution. A constant volume of the solution was taken from the standard solution and poured into several 5 mL graduated flasks containing various amounts of $Bu_4N^+CN^-$. The concentration of Mn(T^{i}PrP)Cl for the UV−vis measurement was maintained at 9.7 μM. ^{1}H and ^{13}C NMR spectra were taken on a JEOL LA300 spectrometer operating at 300.4 MHz for ^{1}H. Chemical shifts were referenced to the residual peaks of deuterated solvents, CD_3OD (δ = 3.30 ppm for ^{1}H, δ = 49.0 ppm for ^{13}C), $CDCl_3$ (7.24, 77.0), CD_2Cl_2 (5.32, 53.8), DMSO-d_6 (2.49, 39.5), DMF-d_7 (2.70, 35.2), $(CD_3)_2CO$ (2.04, 29.8), CD_3CN (1.93, 118.2), and C_6D_6 (7.15, 128.0). For ^{1}H NMR measurement, a 7.5 mM CD_2Cl_2 standard solution of Mn(T^{i}PrP)Cl was prepared. In each measurement, a 550 μL CD_2Cl_2 solution was taken from the standard solution and poured into NMR sample tube under argon atmosphere. An ^{1}H NMR spectrum was taken at 25 °C each time after the addition of certain amount of $Bu_4N^+CN^-$ as a CD_2Cl_2 solution. The ^{13}C NMR spectrum of [Mn(T^{i}PrP)(CN)$_2$]Bu_4N^+ was measured at 25 °C by the addition of 6.0 equiv of $Bu_4N^+CN^-$ to a C_6D_6 solution containing 20 mg of Mn(T^{i}PrP)Cl.

Effective Magnetic Moments. The effective magnetic moment (μ_1^{eff}) of [Mn(T^{i}PrP)(CN)$_2$]$^-Bu_4N^+$ was determined by the Evans method at 25 °C relative to the well-characterized high-spin Mn(T^{i}PrP)Cl complex according to $\mu_1^{eff} = (\Delta\nu_1/\Delta\nu_2)^{1/2}\mu_2^{eff}$, where $\Delta\nu_1$ and $\Delta\nu_2$ are the difference in chemical shifts of the reference signals in [Mn(T^{i}PrP)(CN)$_2$]$^-Bu_4N^+$ and [Mn(T^{i}PrP)Cl], respectively.[18] The effective magnetic moment (μ_1^{eff}) of Mn(T^{i}PrP)(CN) was similarly determined at 25 °C.

Results and Discussion

Reactions of Mn(T^{i}PrP)Cl with $Bu_4N^+CN^-$ in Various Solvents. Titrations of Mn(T^{i}PrP)Cl with $Bu_4N^+CN^-$ have been monitored in various solvents both by UV−vis spectroscopy in a low concentration range, 9.7 μM, and by ^{1}H NMR spectroscopy in a high concentration range, 7.5 mM. Tables 1 and 2 list the absorption maxima (λ_{max}, nm) and chemical shifts (δ, ppm), respectively, for Mn(T^{i}PrP)Cl, Mn(T^{i}PrP)(CN), and [Mn(T^{i}PrP)(CN)$_2$]$^-$ determined in various solvents at 25 °C.

(1) UV−Visible Spectroscopy. (i) Benzene Solution. Figure 1a shows the spectral change observed in benzene solution when $Bu_4N^+CN^-$ was added up to 4.0 equiv relative to Mn(T^{i}PrP)Cl. In the absence of $Bu_4N^+CN^-$, the green Mn(T^{i}PrP)Cl solution showed the absorption bands at 331, 373, 401, 481, 545, 600, and 639 nm. As the $Bu_4N^+CN^-$ solution was added, the signals of Mn(T^{i}PrP)Cl decreased and those of the new complex (**A**) at 334, 385, 407, 494, and 656 nm increased in intensity with the isosbestic points at 373, 445, 489, 531, and 646 nm. After the addition of 4.0 equiv of $Bu_4N^+CN^-$, the green solution showed only the signals for **A**. Figure 1b shows the spectral change observed when much larger amounts of $Bu_4N^+CN^-$, 4.0−1000 equiv, were added to the solution. As the $Bu_4N^+CN^-$ solution was added, the signal intensities for **A** weakened and those of the new complex (**B**) at 339, 414, 440, 464, 551, 585, and 711 nm strengthened with the isosbestic points at 405, 475, 524, 597, and 692 nm. By the addition of a large excess of $Bu_4N^+CN^-$, the signals for **A** completely disappeared and the resultant red solution exhibited only the signals for **B**. Thus, it is most reasonable to consider that the reaction in

(18) Evans, D. F.; James, T. A. *J. Chem. Soc., Dalton Trans.* **1979**, 723−726.

Table 2. ^{1}H NMR Chemical Shifts (δ/ppm, 25 °C) of Mn(Por)Cl (S), Mn(Por)(CN) (mono), and $[Mn(Por)(CN)_2]^-$ (bis)

	pyrrole-H			CH or *ortho*			CH_3 or *meta*		
solvents	S	mono	bis	S	mono	bis	S	mono	bis
				T^{i}PrP					
CD_2Cl_2	−19.4	−23.8	−18.7[d]	9.5	9.3	−1.3[d]	3.2	3.2	−1.3[d]
$CDCl_3$	−19.1	−23.5	*a*	9.8	9.4	*a*	3.3	3.3	*a*
C_6D_6	−13.1	*a*	−17.2	8.9	*a*	−1.1	3.0	*a*	−2.4
DMSO-d_6	−29.3[c]	*a*	−17.7	ca. 4[c]	*a*	−0.6	1.8[c]	*a*	−2.4
CD_3OD	−31.6[c]	*a*	*a*	*b*	*a*	*a*	2.1[c]	*a*	*a*
				TPP					
CD_2Cl_2	−21.9	−28.1	−14.7	*b*	*b*	4.4	8.3	8.2	5.6
$CDCl_3$	−22.5	−28.3	−17.5[d]	*b*	*b*	4.6[d]	8.2	8.2	5.9[d]
C_6D_6	−19.2	−26.6	−14.4	*b*	*b*	4.1	8.0	*b*	5.4
DMSO-d_6	−27.4[c]	*a*	−14.8	8.6[c]	*a*	4.2	7.9[c]	*a*	5.6
CD_3OD	−30.8[c]	−26.2	*a*	9.3[c]	8.5	*a*	7.4[c]	7.4	*a*
				p-CF_3-TPP					
CD_2Cl_2	−21.9	*a*	−14.7	*b*	*a*	4.8	8.6	*a*	5.9
$CDCl_3$	−22.5	−28.1	−15.4	*b*	*b*	4.3	8.6	8.4	5.7
C_6D_6	−19.3	*a*	−14.5	*b*	*a*	4.3	8.2	*a*	5.8
DMSO-d_6	−27.4[c]	*a*	−14.9	8.7[c]	*a*	4.6	7.9[c]	*a*	6.1
CD_3OD	−31.0[c]	*b*	−20.1[d]	9.5[c]	*b*	6.4[d]	7.7[c]	*b*	6.9[d]

[a] Not formed. [b] Too broad. [c] $[Mn(Por)(solvent)_2]^+$. [d] Chemical shifts of the mixture containing some amount of the mono-adduct.

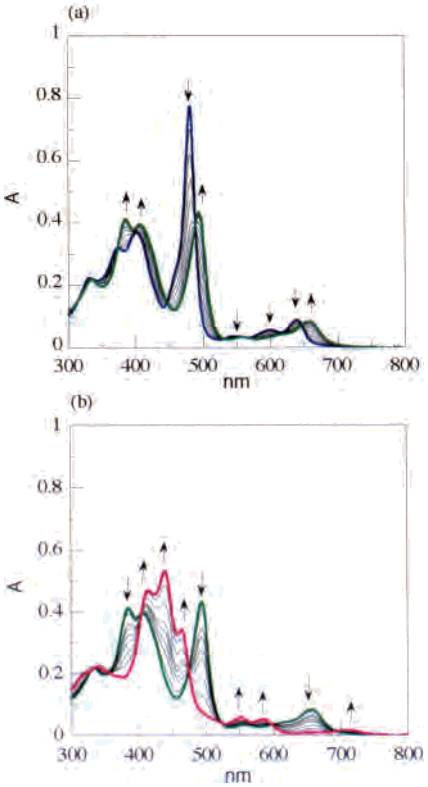

Figure 1. (a) UV−vis spectral change observed when 0−4 equiv of $Bu_4N^+CN^-$ was added to a benzene solution of Mn(T^{i}PrP)Cl at ambient temperature. The blue line is the UV−vis spectrum of Mn(T^{i}PrP)Cl, and the green line is that of [Mn(T^{i}PrP)(CN)] obtained by the addition of 4 equiv of $Bu_4N^+CN^-$. (b) UV−vis spectral change observed when 4−1000 equiv of $Bu_4N^+CN^-$ was added to a benzene solution of Mn(T^{i}PrP)Cl at ambient temperature. The green and red lines correspond to the spectra of [Mn(T^{i}PrP)(CN)] and $[Mn(T^iPrP)(CN)_2]^-$, respectively.

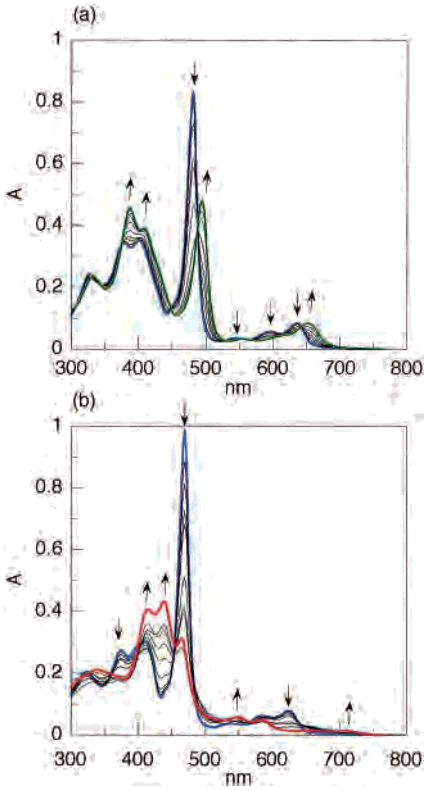

Figure 2. UV−vis spectral change observed when $Bu_4N^+CN^-$ was added to (a) $CHCl_3$ and (b) DMSO solutions of Mn(T^{i}PrP)Cl at ambient temperature. The blue line shows the UV−vis spectrum of the starting complex, Mn(T^{i}PrP)Cl in (a) and $[Mn(T^iPrP)(DMSO)_2]^+$ in (b). Green and red lines are the UV−vis spectra of Mn(T^{i}PrP)(CN), and $[Mn(T^iPrP)(CN)_2]^-$, respectively.

Figure 1a corresponds to the conversion of Mn(T^{i}PrP)Cl to the mono-adduct (**A**), and that in Figure 1b corresponds to the conversion of **A** to the bis-adduct (**B**).

(ii) Dichloromethane Solution. Similar spectral change was observed in CH_2Cl_2 solution, although much larger amounts of $Bu_4N^+CN^-$, at least 10 and 20000 equiv, were necessary for the complete conversion from Mn(T^{i}PrP)Cl to the mono-adduct and from the mono- to the bis-adduct, respectively.

(iii) Chloroform Solution. Figure 2a shows the spectral change observed when $Bu_4N^+CN^-$ was added to the $CHCl_3$ solution of Mn(T^{i}PrP)Cl. Complete conversion from Mn(T^{i}PrP)Cl to the mono-adduct was observed when 10 equiv of $Bu_4N^+CN^-$ was added. No further change was observed, however, even by the addition of 7000 equiv of $Bu_4N^+CN^-$. Thus, the result in $CHCl_3$ solution is quite different from

that in CH_2Cl_2 solution where 78% of the monoadduct is converted to the bis-adduct in the presence of 7000 equiv of $Bu_4N^+CN^-$.

(iv) Dimethyl Sulfoxide Solution. Figure 2b shows the spectral change observed when $Bu_4N^+CN^-$ was added to the DMSO solution of Mn(T^iPrP)Cl. In the absence of $Bu_4N^+CN^-$, the UV−vis spectrum was quite different from the corresponding spectra taken in other solvents such as benzene, CH_2Cl_2, and $CHCl_3$; the intense band at 480 nm in CH_2Cl_2 solution showed a hypsochromic shift to 469 nm in DMSO solution. The difference should be ascribed to the formation of [Mn(T^iPrP)$(DMSO)_2$]Cl in DMSO solution. In fact, the absorption maxima are quite close to those of analogous [Mn(TPP)$(DMSO)_2$]Cl reported previously by Hansen and Goff;[8] the latter complex was formed when Mn(TPP)Cl was dissolved in DMSO. By the addition of $Bu_4N^+CN^-$, the new signals at 414, 438, and 549 nm ascribed to the bis-adduct increased in intensity. The result indicates that the conversion from [Mn(TPP)$(DMSO)_2$]Cl to the bis-adduct took place without accumulation of the mono-adduct. Existence of a small amount of the mono-adduct could not be ruled out; however, since no clear isosbsetic points were observed during the titration process. Similar spectral change was observed in DMF and acetonitrile solutions though the signals for the mono-adduct were observed during the titration process.

(v) Methanol Solution. The UV−vis spectrum of Mn(T^iPrP)Cl taken in methanol solution was quite different from the corresponding spectra taken in benzene, CH_2Cl_2, and $CHCl_3$. Thus, Mn(T^iPrP)Cl is supposed to be converted to [Mn(T^iPrP)$(CH_3OH)_2$]Cl in methanol solution. In fact, the UV−vis spectrum is quite similar to that of [Mn(TPP)$(CH_3OH)_2$]Cl reported previously.[19] The spectrum showed little change even by the addition of 1000 equiv of $Bu_4N^+CN^-$. Thus, it is concluded that neither the mono- nor the bis-adduct was formed in methanol solution.

(2) ^{1}H NMR Spectroscopy. (i) Benzene Solution. Titration of Mn(T^iPrP)Cl with $Bu_4N^+CN^-$ in C_6D_6 solution was hampered due to the extremely low solubility of Mn(T^iPrP)Cl. A clear solution was obtained, however, when 6.0 equiv of $Bu_4N^+CN^-$ was added. The sharp pyrrole signal was observed at δ −17.2 ppm ($\Delta\nu_{1/2}$ = 13 Hz), together with the methyl and methine signals at −2.4 ($\Delta\nu_{1/2}$ = 16 Hz) and −1.1 ppm ($\Delta\nu_{1/2}$ = 28 Hz), respectively. Further addition of the ligand caused no appreciable change in the position and width of each signal. Thus, these signals were ascribed to the bis-adduct. The red color of the solution also supports the formation of the bis-adduct. A similar result was obtained in CCl_4 solution though the complex was very unstable in this solution.

(ii) Dichloromethane Solution. Figure 3 shows the ^{1}H NMR spectral change observed when $Bu_4N^+CN^-$ was added to the CD_2Cl_2 solution of Mn(T^iPrP)Cl. By the addition of 0.5 equiv of $Bu_4N^+CN^-$, a broad pyrrole signal of Mn(T^iPrP)Cl at δ −19.4 ppm ($\Delta\nu_{1/2}$ = 630 Hz) decreased and a new signal at −23.8 ppm ($\Delta\nu_{1/2}$ = 630 Hz), assigned to the pyrrole signal of the mono-adduct, increased in intensity. The methine and methyl signals showed little change from the original positions. When 1.0 equiv of $Bu_4N^+CN^-$ was added, the signal at −19.4 ppm completely disappeared. The solution color was maintained green. Further addition of $Bu_4N^+CN^-$ caused a gradual downfield shift of the pyrrole signal from −24 to −19 ppm with considerable narrowing. In contrast, the methyl and methine signals showed upfield shifts. When 10 equiv of $Bu_4N^+CN^-$ was added, the pyrrole, methine, and methyl signals were observed at −18.7, −1.3, and −1.3 ppm, respectively, as relatively sharp signals. The solution color became red at this point. These signals showed a little shift on further addition of $Bu_4N^+CN^-$. Complete conversion to the bis-addcut was not achieved, however, even by the addition of 15 equiv of $Bu_4N^+CN^-$ as is revealed from a rather broad pyrrole signal. Thus, the spectrum in Figure 3f shows a mixture consisting of bis- and mono-adduct in 3:1 ratio; the ratio was estimated under the assumption that chemical shifts for the mono- and bis-adduct are −23.5 and −17.2 ppm, respectively. The fact that the only one pyrrole signal was observed during the titration process suggests that the ligand exchange between the mono- and bis-adduct is fast on the ^{1}H NMR time scale at least at 25 °C.

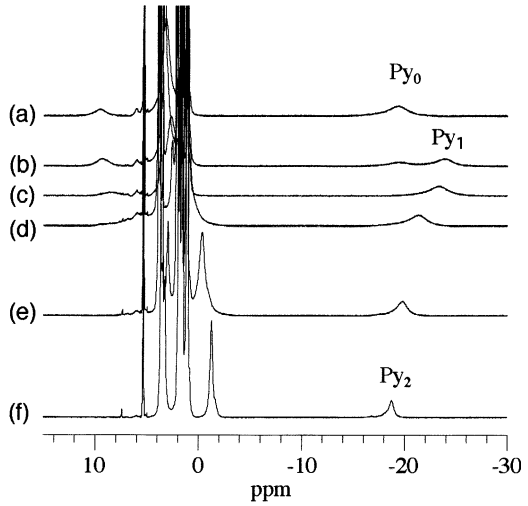

Figure 3. ^{1}H NMR spectral change observed when (a) 0, (b) 0.5, (c) 1.0, (d) 2.0, (e) 4.0, and (f) 10.0 equiv of $Bu_4N^+CN^-$ was added to a CD_2Cl_2 solution of Mn(T^iPrP)Cl at 25 °C.

(iii) Chloroform Solution. Figure 4 shows the ^{1}H NMR spectral change observed when $Bu_4N^+CN^-$ was added to the $CDCl_3$ solution of Mn(T^iPrP)Cl. As in the case of the CD_2Cl_2 solution mentioned above, a broad signal at δ −19.1 ppm weakened and a new signal at −23.5 ppm increased in intensity. No further spectral change was observed, however, even by the addition of 15 equiv of $Bu_4N^+CN^-$. In addition, the solution color was maintained green. The results strongly indicate that, contrary to the reaction in CD_2Cl_2, the mono-adduct is the only product in $CDCl_3$ solution.

(iv) Dimethyl Sulfoxide Solution. Figure 5 shows the ^{1}H NMR spectral change observed when $Bu_4N^+CN^-$ was added to the DMSO-d_6 solution of Mn(T^iPrP)Cl. The pyrrole, methine, and methyl signals of Mn(T^iPrP)Cl appeared at −29.3, ca. 4, and 1.8 ppm, respectively, at 25 °C. Thus, the

(19) Hatano, K.; Anzai, K.; Iitaka, Y. *Bull. Chem. Soc. Jpn.* **1983**, *56*, 422−427.

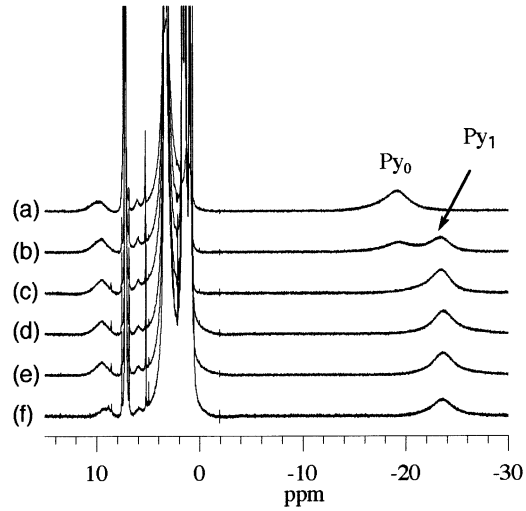

Figure 4. ^{1}H NMR spectral change observed when (a) 0, (b) 0.5, (c) 1.0, (d) 1.5, (e) 2.0, and (f) 15.0 equiv of $Bu_4N^+CN^-$ was added to a $CDCl_3$ solution of Mn(T^{i}PrP)Cl at 25 °C.

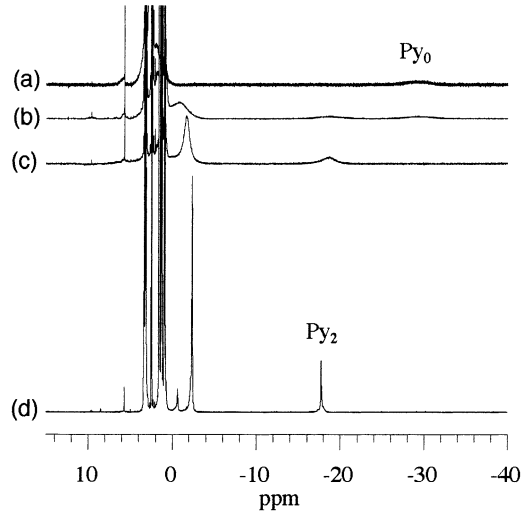

Figure 5. ^{1}H NMR spectral change observed when (a) 0, (b) 1.0, (c) 2.0, and (d) 10.0 equiv of $Bu_4N^+CN^-$ was added to a DMSO-d_6 solution of Mn(T^{i}PrP)Cl at 25 °C.

chemical shifts are quite different from those determined in other solvents such as CD_2Cl_2, $CDCl_3$, and C_6D_6; the pyrrole, methine, and methyl signals appeared at −19.4, 9.5, and 3.2 ppm, respectively, in CD_2Cl_2 solution at 25 °C. As mentioned in the UV−vis section, the difference in chemical shifts should be ascribed to the formation of $[Mn(T^iPrP)(DMSO)_2]$-Cl in DMSO solution rather than to the solvent effect on the chemical shifts of Mn(T^{i}PrP)Cl.[8] When 1.0 equiv of $Bu_4N^+CN^-$ was added, the signals for the starting complex decreased and those for the product increased in intensity; the product showed a broad pyrrole signal at −18.4 ppm. When 2.0 equiv of $Bu_4N^+CN^-$ was added, the pyrrole signal of the starting complex completely disappeared and that of the product increased in intensity. Further addition of $Bu_4N^+CN^-$ sharpened each signal without considerable change in its position; the pyrrole, methine, and methyl signals were observed at −17.7 ($\Delta\nu_{1/2} = 26$ Hz), −0.6 ($\Delta\nu_{1/2} = 33$ Hz), and −2.4 ($\Delta\nu_{1/2} = 17$ Hz) ppm, respectively, when 12 equiv of $Bu_4N^+CN^-$ was added. The originally green solution turned red at this point. The spectral change mentioned above indicates that the major product is the bis-adduct even by the addition of 1.0 equiv of $Bu_4N^+CN^-$. The broad pyrrole signal for the bis-adduct, observed when 1.0−4.0 equiv of $Bu_4N^+CN^-$ was added, suggests that a small amount of the mono-adduct also exists in the solution and involves in the fast ligand exchange with the bis-adduct. Thus, the spectral change observed by ^{1}H NMR spectroscopy is totally consistent with that observed by UV−vis spectroscopy. Titration experiments in other dipolar aprotic solvents such as acetonitrile, DMF, and acetone were difficult due to the low solubility of Mn(T^{i}PrP)Cl in these solvents. A clear red solution was obtained in each case, however, by the addition of 6 equiv of $Bu_4N^+CN^-$, which exhibited the sole entity of the bis-adduct as revealed from the chemical shift and the signal width. On the basis of these results, it is concluded that the bis-adduct is preferentially formed in dipolar aprotic solvents even when $Bu_4N^+CN^-$ is less than 2.0 equiv.

(v) Methanol Solution. As in the case of the DMSO solution mentioned above, the chemical shifts in methanol solution are quite different from those determined in less polar solvents such as CD_2Cl_2, $CDCl_3$, and C_6D_6. Thus, Mn(T^{i}PrP)Cl is converted to $[Mn(T^iPrP)(CD_3OD)_2]Cl$ in methanol solution. No appreciable change was observed in the ^{1}H NMR spectrum even by the addition of 15 equiv of $Bu_4N^+CN^-$. The result clearly indicates that neither the mono- nor the bis-adduct is formed in methanol solution in the presence of a large excess of $Bu_4N^+CN^-$.

(3) Formation Constants for the Mono- and Bis-Adducts. The formation constants K_1 and K_2 corresponding to eqs 1 and 2, respectively, were determined by the UV−vis spectroscopy at 25 °C according to the method of Rossotti and Rossotti.[7,20,21]

$$Mn(T^iPrP)Cl + Bu_4N^+CN^- \rightleftarrows Mn(T^iPrP)(CN) + Bu_4N^+Cl^- \quad (1)$$

$$Mn(T^iPrP)(CN) + Bu_4N^+CN^- \rightleftarrows [Mn(T^iPrP)(CN)_2]^-Bu_4N^+ \quad (2)$$

In benzene solution, the K_1 and K_2 values were determined as follows on the basis of the spectral change given in Figure 1a,b, respectively: $K_1 = 15$ and $K_2 = 1600$ M^{-1}. The formation constants in CH_2Cl_2 solution were similarly determined as $K_1 = 46$ and $K_2 = 23$ M^{-1}. In $CHCl_3$ solution, the K_1 value was determined as $K_1 = 0.96$. Because the bis-adduct was not observed even by the addition of 7000 equiv of $Bu_4N^+CN^-$, we estimated the K_2 value to be less than 0.8 M^{-1} by assuming the 5% conversion from the mono- to the bis-adduct in the presence of 7000 equiv of $Bu_4N^+CN^-$. As mentioned, Mn(T^{i}PrP)Cl is converted to the six-coordinated complexes, $[Mn(T^iPrP)(Solv)_2]Cl$, in polar solvents such as DMSO and CH_3OH. Thus, the formation constants in these solvents were not determined.

(20) Rossotti, F. J. C.; Rossotti, H. In *The Determination of Stability Constants*; McGraw-Hill: New York, 1961; p 277.
(21) Neya, S.; Morishima, I.; Yonezawa, T. *Biochemistry* **1981**, *20*, 2610−2614.

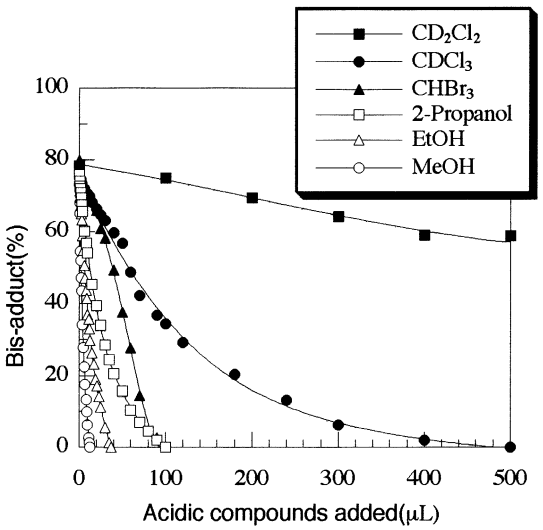

Figure 6. Decrease in the population ratios of $[Mn(T^iPrP)(CN)_2]^-$ observed when the compounds with proton-donating ability were added to the CD_2Cl_2 solution consisting of $[Mn(T^iPrP)(CN)_2]^-$ (76%) and $Mn(T^iPrP)(CN)$ (24%).

Solvent Effects on the Mono/Bis Ratios. The UV−vis and ^{1}H NMR results described above indicate that the reaction products are greatly influenced by the solvents used: (i) The reactions in dipolar aprotic solvents such as DMSO, DMF, acetone, acetonitrile, and nitromethane yielded preferentially the bis-adduct. (ii) The reactions in the less polar solvents such as CH_2Cl_2 and benzene yielded both the mono- and bis-adduct depending on the amount of cyanide added, though the complete conversion to the bis-adduct was achieved with much smaller amount of the ligand in benzene solution. (iii) The reaction in $CHCl_3$ formed only the mono-adduct. (iv) The reaction in methanol gave neither the mono- nor the bis-adduct. Thus, the affinity of cyanide toward the Mn(III) ion in $Mn(T^iPrP)Cl$ is larger in nonpolar and dipolar aprotic solvents than in protic solvents. The order of the ligand affinity in various solvents is ranked as given in eq 3.

$$CH_3OH < CHCl_3 < CH_2Cl_2 < (CH_3)_2CO, DMSO, DMF, CH_3CN, C_6H_6, CCl_4 \quad (3)$$

The order in eq 3 could be the suggestion that the solvents with hydrogen donor ability weaken the coordination ability of cyanide ligand.[3] To reveal the effect of hydrogen bonding on the product ratio, we added weak acidic compounds such as methanol, ethanol, 2-propanol, $CHCl_3$, and $CHBr_3$ to the CD_2Cl_2 solution consisting of 76% bis-adduct and 24% mono-adduct. Figure 6 shows how the population ratio of the bis-adduct decreases as the acidic compounds were added. The degree of decrease was quite different depending on the compounds. In the case of methanol, addition of only 7 μL converted the bis-adduct to the mono-adduct to form the solution consisting of 20% bis- and 80% mono-adduct. In contrast, much larger amounts, 18 and 40 μL, were necessary for the same conversion in the case of ethanol and 2-propanol, respectively. Since the pK_a values of methanol, ethanol, and 2-propanol are 15.2, 16.0, and 16.5, respectively,[22] the results indicate that the strength of the O−H···N hydrogen bonding determines the relative population of the mono- and bis-adducts. Similarly, 66 and 180 μL of $CHBr_3$ and $CHCl_3$ were necessary, respectively, to obtain the solution containing 20% bis-adduct and 80% mono-adduct. Thus, the coordination ability of cyanide increases as the solvent changes from CH_3OH to $CHCl_3$ as given in eq 4. Since $CHBr_3$ is known to be a much stronger hydrogen donor in the C−H···N intermolecular hydrogen bonding,[23] the results again indicate that the O−H···N and C−H···N hydrogen bonding plays an important role to determine the coordination structure of the products.

$$CH_3OH < CH_3CH_2OH < (CH_3)_2CHOH < CHBr_3 < CHCl_3 \quad (4)$$

On the basis of the discussion given above, the coordination ability of cyanide toward Mn(III) can be summarized as follows. In nonpolar or dipolar aprotic solvents where no hydrogen bonding occurs between cyanide and solvent molecules, cyanide behaves as a strong ligand and forms the bis-adduct. In $CHCl_3$ solution, however, the C−H···N hydrogen bonding weakens the coordination ability of the cyanide ligand. As a result, cyanide behaves as a much weaker anionic ligand such as halide to form preferentially the mono-adduct. In methanol solution, strong O−H···N hydrogen bonding further weakens the coordination ability of cyanide to such an extent as to make the ligand substitution difficult to occur. To further confirm the validity of the above-mentioned speculation, we have examined the coordination ability of *tert*-butyl isocyanide (^{t}BuNC). Because the electronic structure of ^{t}BuNC is considered to be quite similar to the cyanide with a strong hydrogen bonding,[4,5,24] the coordination of ^{t}BuNC toward Mn(Por)Cl must be very weak. As expected, no coordination was observed even by the addition of 20 equiv of ^{t}BuNC to $Mn(T^iPrP)Cl$ in CD_2Cl_2 solution.

Comparison of Porphyrins. We have then examined the population ratios of the mono- and bis-adduct by using Mn(TPP)Cl. The reaction products were analyzed by ^{1}H NMR spectroscopy. The chemical shifts of the mono- and bis-adducts, Mn(TPP)(CN) and $[Mn(TPP)(CN)_2]^-$, in various solvents are listed in Table 2b together with those of Mn(TPP)Cl. The most characteristic point is that the ratio of the bis-adduct relative to the corresponding mono-adduct increases in each solvent on going from T^iPrP to TPP complexes. Thus, while the bis-adduct was not formed in $CDCl_3$ solution in the case of $Mn(T^iPrP)Cl$ even by the addition of 15 equiv of $Bu_4N^+CN^-$, 73% of the bis-adduct was formed in the case of Mn(TPP)Cl under the same condition. Similarly, while no adduct was formed in CD_3OD solution in the case of $[Mn(T^iPrP)(CD_3OD)_2]Cl$ even by the addition of 15 equiv of $Bu_4N^+CN^-$, mono-adduct was

(22) Reeve, W.; Erikson, C. M.; Aluotto, P. F. *Can. J. Chem.* **1979**, *57*, 2747−2754.
(23) Allerhand, A.; Schleyer, P. von R. *J. Am. Chem. Soc.* **1963**, *85*, 1715−1723.
(24) Simonneaux, G.; Hindre, F.; Pouzennec, M. L. *Inorg. Chem.* **1989**, *28*, 823−825.

actually formed in the case of $[Mn(TPP)(CD_3OD)_2]Cl$ under the same conditions; formation of the bis-adduct was not observed in this condition. As mentioned in the Introduction, Sheidt and co-workers reported the formation of the bis-adduct $[Mn(TPP)(CN)_2]^-$ in methanol solution on the basis of UV−vis spectroscopic results.[7] The discrepancy should be ascribed to the difference in the molar ratios of cyanide relative to the complex; ca. 18 000 equiv of K^+CN^- was added relative to Mn(TPP)(OH) in UV−vis measurement,[7] while 15 equiv of $Bu_4N^+CN^-$ was added relative to Mn(TPP)Cl in the ^1H NMR experiment. The difference in product ratio between $CDCl_3$ and CD_2Cl_2 solutions was also clearly shown in Mn(TPP)Cl. While the addition of 2 equiv of $Bu_4N^+CN^-$ produced more than 90% of the bis-adduct in CD_2Cl_2, only 16% of the bis-adduct was formed in $CDCl_3$. The difference in product ratios between two porphyrin complexes should be ascribed to the steric and electronic effects of the *meso* substituents. Because of the presence of bulky isopropyl group, the porphyrin ring is supposed to be strongly ruffled as in the case of the Fe(III) complexes such as Fe(T^{i}PrP)Cl and $[Fe(T^iPrP)(THF)_2]ClO_4$.[25,26] As a result, the Mn(III)−N(porphyrin) bonds must be shortened, resulting in the strong electron donation of the porphyrin nitrogen atoms toward the central Mn(III) ion. The presence of the electron-donating alkyl groups also contributes to the strong coordination of the porphyrin nitrogen atoms. The intense equatorial coordination in Mn(T^{i}PrP)Cl could, in turn, weaken the axial coordination of cyanide ligand toward Mn(T^{i}PrP)Cl as compared toMn(TPP)Cl.

The results indicate that the population ratio of the bis-adduct could further increase in Mn(*p*-CF_3-TPP)Cl due to the presence of strong electron-withdrawing substituents at the *meso*-phenyl groups. In fact, even by the addition of 2.0 equiv of $Bu_4N^+CN^-$, 78% of the bis-adduct was formed in $CDCl_3$ solution; the population ratio of the bis-adduct was only 16% in the case of Mn(TPP)Cl under the same condition. Table 2c lists the chemical shifts of these complexes taken in various solvents. Figure 7 shows how the relative population of the bis-adduct changes among different porphyrin complexes in $CDCl_3$ solution by the addition of $Bu_4N^+CN^-$. The data for Mn(TMP)Cl and Mn(2,6-Cl_2-TPP)Cl are also added in Figure 7. Clearly, binding of cyanide toward Mn(III) ions increase in the order given in eq 5.

$$\text{Mn(T}^i\text{PrP)Cl, Mn(TMP)Cl} < \text{Mn(TPP)Cl, Mn(2,6-Cl}_2\text{-TPP)Cl} < \text{Mn(}p\text{-CF}_3\text{-TPP)Cl} \quad (5)$$

Electronic States of Mono- and Bis-Adducts of Manganese Complexes. It is well-known that five-coordinated manganese(III) porphyrin complexes with anionic ligands (X) such as halides, hydroxide, and cyanide show the high-spin ($S = 2$) state.[27,28] In the present case, we have determined

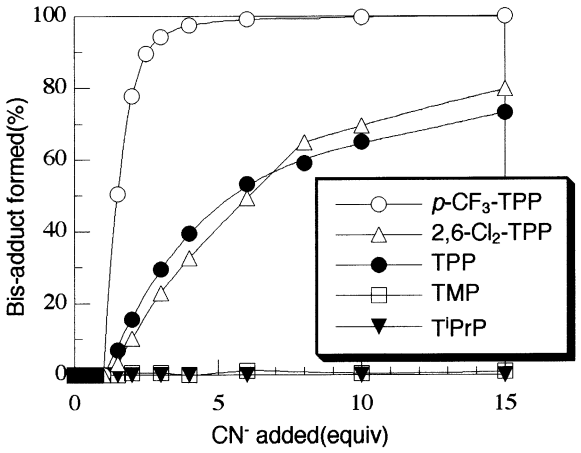

Figure 7. Increase in the population ratios of $[Mn(T^iPrP)(CN)_2]^-$ observed when $Bu_4N^+CN^-$ was added to the $CDCl_3$ solutions of various Mn(Por)Cl, where Por's are T^{i}PrP, TMP, TPP, *p*-CF_3-TPP, and 2,6-Cl_2-TPP.

the effective magnetic moment of Mn(T^{i}PrP)(CN) by the Evans method in $CHCl_3$; the pure complex can be obtained in this solution simply by the addition of an excess amount of $Bu_4N^+CN^-$ to Mn(T^{i}PrP)Cl. The effective magnetic moment was 5.0 μ_B at 25 °C, which indicates that the complex is in the $S = 2$ spin state. Six-coordinated Mn(III) porphyrin complexes with strong axial ligands such as $[Mn(TPP)(CN)_2]^-K^+$ and $[Mn(TPP)(Im)_2]^-K^+$ (Im: imidazolate) are reported to exhibit the low-spin ($S = 1$) state.[8] We are extremely interested in the spin state of $[Mn(T^iPrP)(CN)_2]^-$ because the analogous low-spin iron(III) complex $[Fe(T^iPrP)(CN)_2]^-$ shows a less common $(d_{xz}, d_{yz})^4(d_{xy})^1$ electron configuration due to the highly ruffled porphyrin structure;[29−32] recent studies have revealed the general conditions to determine the electron configurations of the low-spin Fe(III) porphyrin complexes.[33−39] If presumably ruffled $[Mn(T^iPrP)(CN)_2]^-$ shows the reversal of the energy levels between the (d_{xz}, d_{yz}) and d_{xy} orbitals as in the case of the corresponding Fe(III) complex, then the Mn(III) complex should be diamagnetic with the $(d_{xz}, d_{yz})^4(d_{xy})^0$ electron configuration. This expectation was not realized because

(25) Ikeue, T.; Ohgo, Y.; Uchida, A.; Nakamura, M.; Fujii, H.; Yokoyama, M. *Inorg. Chem*. **1999**, *38*, 1276−1281.
(26) Ohgo, Y.; Saitoh, T.; Nakamura, M. *Acta Crystallogr*. **2001**, *C57*, 233−234.
(27) Goff, H. M.; Hansen, A. P. *Inorg. Chem.* **1984**, *23*, 321−326.
(28) Turner, P.; Gunter, M. J. *Inorg. Chem.* **1994**, *33*, 1406−1415.
(29) Nakamura, M.; Ikeue, T.; Fujii, H.; Yoshimura, T. *J. Am. Chem. Soc*. **1997**, *119*, 6284−6291.
(30) Nakamura, M.; Ikeue, T.; Fujii, H.; Yoshimura, T.; Tajima, K. *Inorg. Chem*. **1998**, *37*, 2405−2414.
(31) Ikeue, T.; Ohgo, Y.; Saitoh, T.; Nakamura, M.; Fujii, H.; Yokoyama, M. *J. Am. Chem. Soc*. **2000**, *122*, 4068−4076.
(32) Ikeue, T.; Ohgo, Y.; Saitoh, T.; Yamaguchi, T.; Nakamura, M. *Inorg. Chem*. **2001**, *40*, 3423−3434.
(33) Walker, F. A.; Simonis, U. Proton NMR Spectroscopy of Model Hemes. In *NMR of Paramagnetic Molecules*; Berliner, L. J., Reuben, J., Eds.; Biological Magnetic Resonance Vol. 12; Plenum Press: New York, 1993; pp 133−274.
(34) Walker, F. A. In *The Porphyrin Handbook*; Kadish, K. M., Smith, K. M., Guilard, R., Eds.; Academic Press: San Diego, CA, 2000; Vol. 5, Chapter 36, pp 81−183.
(35) Wołowiec, S.; Latos-Grażyński, L.; Mazzanti, M.; Marchon, J.-C. *Inorg. Chem*. **1997**, *36*, 5761−5771.
(36) Pilard, M.-A.; Guillemot, M.; Toupet, L.; Jordanov, J.; Simonneaux, G. *Inorg. Chem*. **1997**, *36*, 6307−6314.
(37) Wołowiec, S.; Latos-Grażyński, L.; Toronto, D.; Marchon, J.-C. *Inorg. Chem*. **1998**, *37*, 724−732.
(38) Nakamura, M.; Ikeue, T.; Ikezaki, A.; Ohgo, Y.; Fujii, H. *Inorg. Chem*. **1999**, *38*, 3857−3862.
(39) Simonneaux, G.; Schünemann, V.; Morice, C.; Carel, L.; Toupet, L.; Winkler, H.; Trautwein, A. X.; Walker, F. A. *J. Am. Chem. Soc*. **2000**, *122*, 4366−4377.

Table 3. ^{13}C NMR Chemical Shifts (δ/ppm) of Complexes Determined at 25 °C

complexes	solvents	α-pyrrole	β-pyrrole	meso	−CH	$-CH_3$
$[Mn(T^iPrP)(CN)_2]^-$	C_6D_6	293	−53	141	39.7	85.8
$Mn(T^iPrP)(CN)$	$CDCl_3$	503	−137	211	42.6	119.0
$Mn(T^iPrP)Cl$	$CDCl_3$	484	−157	220	44.8	113.4
	CD_2Cl_2	475	−153	216	47.9	112.5
	DMSO-d_6[a]	490	−223	102	43.7	90.5
	CD_3OD[b]	517	−238	113	41.6	99.0

[a] $[Mn(T^iPrP)(DMSO)_2]^+$. [b] $[Mn(T^iPrP)(CD_3OD)_2]^+$.

$[Mn(T^iPrP)(CN)_2]^-$ showed a paramagnetically shifted pyrrole signal at −17.2 ppm in benzene solution. In fact, the effective magnetic moment of $[Mn(T^iPrP)(CN)_2]^-$ determined by the Evans method in benzene solution was 3.2 μ_B at 25 °C, indicating that the complex is in the low-spin ($S = 1$) state with the $(d_{xy})^2(d_{xz}, d_{yz})^2$ electron configuration as in the case of the other low-spin Mn(III) complex. Hansen and Goff reported the unpaired spin densities centered on the π MO of the carbon atoms in $[Mn(TPP)(CN)_2]^-$ on the basis of the ^{1}H NMR chemical shifts.[8] Although both $[Mn(T^iPrP)(CN)_2]^-$ and $[Mn(TPP)(CN)_2]^-$ are in the $S = 1$ spin state, the π spin distribution on the porphyrin carbons in $[Mn(T^iPrP)(CN)_2]^-$ could be different from that in $[Mn(TPP)(CN)_2]^-$ due to the highly ruffled structure in the former complex. To reveal the effect of porphyrin deformation on the π spin densities at the porphyrin carbon atoms, the data for both the ^{1}H and ^{13}C NMR chemical shifts are necessary. Thus, we have measured the ^{13}C NMR chemical shifts of $[Mn(T^iPrP)(CN)_2]^-$ and listed them in Table 3 together with those of $Mn(T^iPrP)(CN)$ and $Mn(T^iPrP)Cl$. To determine the spin densities, we have separated the ^{1}H NMR isotropic shift (δ_{iso}) into dipolar shift (δ_{dip}) and contact shift(δ_{con}) by using the chemical shifts of the corresponding diamagnetic cobalt(III) complex $[Co(T^iPrP)(CN)_2]^-$ as δ_{dia} values.[40−44] The metal-centered dipolar shift in the complexes with axial symmetry is defined by eq 6, where χ values are molecular susceptibilities and the term $(3\cos^2\theta - 1)/r^3$ is referred to as the axial geometric factor:

$$\delta_{dip}{}^{MC} = (1/12\pi)(\chi_{||} - \chi_{\perp})(3\cos^2\theta - 1)/r^3 \qquad (6)$$

In the case of $[Mn(T^iPrP)(CN)_2]^-$, we have determined the dipolar shifts of the pyrrole and isopropyl CH protons by assuming that the isotropic shift of the isopropyl CH_3 protons is totally ascribed to the dipolar shift. The contact shift of each proton is then obtained by $\delta_{con} = \delta_{iso} - \delta_{dip}$. Once the contact shift is determined, the proton hyperfine coupling constant, A^H, can be calculated by

$$\delta_{con} = (A^H)|\gamma_e/\gamma_H|S(S+1)/(3kT) \qquad (7)$$

Because the proton hyperfine coupling constant is proportional to the spin density ρ^π of the carbon atom to which the proton is attached, it is possible to determine the spin density at the carbon by

$$A^H/h = (Q^H{}_{CH}\rho^\pi)/2S \qquad (8)$$

where $Q^H{}_{CH}$ is a proportional constant.[45,46] The π spin density of the β-pyrrole carbon atoms was estimated as +0.0066 by the use of $Q^H{}_{CH} = -65.8$ MHz in eq 8.[44,47]

To determine the π spin densities at the α-pyrrole and *meso*-carbon as well as pyrrole nitrogen atoms, analysis of the ^{13}C NMR chemical shifts is necessary. Carbon-13 isotropic shift is presented by

$$\delta_{iso} = \delta_{dip}{}^{MC} + \delta_{dip}{}^{LC} + \delta_{con} \qquad (9)$$

where $\delta_{dip}{}^{LC}$ is a ligand-centered dipolar shift. Carbon contact shifts originate from unpairing of carbon 1s electrons and unpairing of the three carbon sp^2 bonding pairs. Thus, the contact shift for the β-pyrrole carbon can be expressed by the Karplus and Frankel equation,

$$\delta_{con}(\text{py-}\beta) = [(S^c + 2Q^C{}_{CC'} + Q^C{}_{CH})\rho^\pi{}_\beta + Q^C{}_{C'C}(\rho^\pi{}_\beta + \rho^\pi{}_\alpha)]F^C$$

where $F^C = |\gamma_e/\gamma_C|S(S+1)/(3kT)$.

In the equation, the S^C term indicates polarization of the 1s orbital. The $Q^C{}_{CC'}$ and $Q^C{}_{CH}$ terms reflect polarization of the three sp^2 bonds by π-spin density at the observed carbon atom. The $Q^C{}_{C'C}$ term represents polarization of the C−C bond by π−spin densities centered on the neighboring carbon atoms. The $\delta_{dip}{}^{LC}$ is assumed to be proportional to the spin density ρ^π at the observed carbon atom and is given by $\delta_{dip}{}^{LC} = D\rho^\pi$. Thus, the $(\delta_{dip}{}^{LC} + \delta_{con})$ values for the py-α, py-β, *meso*, and α carbons, which can easily be obtained by $(\delta_{iso} - \delta_{dip}{}^{MC})$, are expressed by eqs 10−13, respectively.

$$\text{py-}\alpha:\ \delta_{con} + \delta_{dip}{}^{LC} = D\rho^\pi{}_{py-\alpha} + [(S^c + 2Q^C{}_{CC'} + Q^C{}_{CN})\rho^\pi{}_{py-\alpha} + Q^C{}_{C'C}(\rho^\pi{}_{py-\beta} + \rho^\pi{}_{meso}) + Q^C{}_{NC}\rho^\pi{}_N]F^C \qquad (10)$$

$$\text{py-}\beta:\ \delta_{con} + \delta_{dip}{}^{LC} = D\rho^\pi{}_{py-\beta} + [(S^c + 2Q^C{}_{CC'} + Q^C{}_{CH})\rho^\pi{}_{py-\beta} + Q^C{}_{C'C}(\rho^\pi{}_{py-\beta} + \rho^\pi{}_{py-\alpha})]F^C \qquad (11)$$

$$\textit{meso}:\ \delta_{con} + \delta_{dip}{}^{LC} = D\rho^\pi{}_{meso} + [(S^c + 3Q^C{}_{CC'})\rho^\pi{}_{meso} + 2Q^C{}_{C'C}\rho^\pi{}_{py-\alpha}]F^C \qquad (12)$$

$$C_\alpha:\ \delta_{con} + \delta_{dip}{}^{LC} = D\rho^\pi C_\alpha + [(S^c + 3Q^C{}_{CC'})\rho^\pi{}_{C\alpha} + Q^C{}_{C'C}\rho^\pi{}_{meso}]F^C \qquad (13)$$

(40) La Mar, G. N.; Walker, F. A. In *The Porphyrins*; Dolphin, D., Ed.; Academic Press: New York, 1979; Vol. IV, pp 61−157.
(41) Goff, H. In *Iron Porphyrins, Part I*; Lever, A. B. P., Gray, H. B., Eds.; Physical Bioinorganic Chemistry Series 1; Addison-Wesley: Reading, MA, 1983; pp 237−281.
(42) Bertini, I.; Luchinat, C. In *NMR of Paramagnetic Molecules in Biological Systems*; Lever, A. B. P., Gray, H. B., Eds.; Physical Bioinorganic Chemistry Series 3; Benjamin/Cummings: Menlo Park, CA, 1986; pp 165−229.
(43) Mispelter, J.; Momenteau, M.; Lhoste, J.-M. Heteronuclear Magnetic Resonance. In *NMR of Paramagnetic Molecules*; Berliner, L. J., Reuben, J., Eds.; Biological Magnetic Resonance Vol. 12; Plenum Press: New York, 1993; pp 299−355.
(44) Bertini, I.; Luchinat, C. In *NMR of Paramagnetic Substances*; Lever, A. B. P., Ed.; Coordination Chemistry Reviews 150; Elsevier: Amsterdam, 1996; pp 29−75.
(45) Heller, C.; McConnell, H. M. *J. Chem. Phys.* **1960**, *32*, 1535.
(46) McLachlan, A. D. *Mol. Phys.* **1958**, *1*, 233−240.
(47) Karplus, M.; Fraenkel, G. K. *J. Chem. Phys.* **1961**, *35*, 1312−1323.

Table 4. Separation of ^{13}C NMR Chemical Shift Terms in $[Mn(T^iPrP)(CN)_2]^-$ in C_6D_6 at 25 °C Together with π Spin Densities[a]

carbons	δ_{obs}	δ_{dia}[b]	δ_{iso}	$\delta^{MC}{}_{dip}$	$\delta^{LC}{}_{dip}$	δcon	$\rho_C{}^{\pi}$
meso	141.0 (11.7)	122.3 (119.1)	18.7 (−107.4)	−32.9 (−23.0)	61.1 (179.3)	−9.5 (−263.7)	−0.0014 (−0.0059)
α-pyrrole	293.0 (374.5)	140.4 (143.4)	152.6 (231.1)	−52.2 (−33.1)	47.8 (−173.0)	157.0 (437.2)	−0.0011 (0.0056)
β-pyrrole	−53.0 (−37.0)	131.2 (133.4)	−184.2 (−170.4)	−19.2 (−12.0)	−288.7 (−217.6)	123.7 (59.2)	0.0066 (0.0071)
CH(ipso)	39.7 (198.7)	34.7 (142.4)	5.0 (56.3)	−10.2 (−7.8)	0.0 (0.0)	15.2 (64.1)	
CH_3	85.8	28.9	56.9	−5.4	0.0	62.3	

[a] Numbers in the parentheses are those of $[Mn(TPP)(CN)_2]^-$. *D* values for $[Mn(T^iPrP)(CN)_2]^-$ and $[Mn(TPP)(CN)_2]^-$ are −44 000 and −31 000, respectively. [b] Chemical shifts of the corresponding carbons in diamagnetic $[Co(T^iPrP)(CN)_2]^-$ and $[Co(TPP)(CN)_2]^-$.

Since $\rho^{\pi}{}_{C\alpha}$ is supposed to be zero, the contact shift value of the methine carbon is given by eq 14.

$$\delta_{con}(C_\alpha) = Q^C{}_{C'C}\rho^{\pi}{}_{meso}F^C \quad (14)$$

The S^C and Q^C values are as follows: $S^C = -35.5$ MHz; $Q^C{}_{CC'} = +40.3$ MHz; $Q^C{}_{CH} = +54.6$ MHz; $Q^C{}_{CN} = +40.3$ MHz; $Q^C{}_{C'C} = -39.0$ MHz; $Q^C{}_{NC} = -39.0$ MHz.[44,47] By putting $\delta_{con}(C_\alpha) = 15.2$ ppm into eq 14, we could determine $\rho^{\pi}{}_{meso} = -0.0014$. Solution of the simultaneous eqs 10−13 using $\rho^{\pi}{}_{meso} = -0.0014$ and $\rho^{\pi}{}_{py-\beta} = 0.0066$ yields $\rho^{\pi}{}_{\alpha}$, $\rho^{\pi}{}_{N}$, and *D* to be −0.0011, −0.022, and −44000, respectively. Table 4 lists the separation of chemical shift terms together with the spin densities of carbon atoms.

The data in Table 4 should be compared with those in $[Mn(Por)(CN)_2]^-$ (Por = TPP and OEP) reported by Hansen and Goff; the $\rho^{\pi}{}_{meso}$ and $\rho^{\pi}{}_{py-\beta}$ values are −0.015 and +0.0076, respectively.[8] Thus, while the $\rho^{\pi}{}_{py-\beta}$ values of the two complexes are quite similar, the spin densities at the *meso* carbon are greatly different; the $\rho^{\pi}{}_{meso}$ value in $[Mn(T^iPrP)(CN)_2]^-$ is only 1/10 of that in $[Mn(Por)(CN)_2]^-$ (Por = OEP). The large negative $\rho^{\pi}{}_{meso}$ value in $[Mn(Por)(CN)_2]^-$ could be the indication that $[Mn(Por)(CN)_2]^-$ has much larger positive π spin densities at the α-pyrrole carbon atoms. To determine the spin densities at the α-pyrrole carbon and nitrogen atoms of $[Mn(TPP)(CN)_2]^-$, we have measured the ^{13}C NMR chemical shifts in C_6D_6 solution at 25 °C and listed them in Table 4. As expected, the α-pyrrole signal appears at 374.5 ppm while the *meso* signal is observed at 11.7 ppm; the α-pyrrole and *meso* signals are observed at 293 and 141.0 ppm, respectively, in the case of $[Mn(T^iPrP)(CN)_2]^-$. The spin densities of $[Mn(TPP)(CN)_2]^-$ are similarly determined on the basis of the ^1H and ^{13}C NMR chemical shifts, and they are also listed in Table 4. The $\rho^{\pi}{}_{py-\beta}$ value is consistent with that reported by Goff and Hansen, though the $\rho^{\pi}{}_{meso}$ value is much smaller; the $\rho^{\pi}{}_{meso}$ value reported by Goff and Hansen was determined on the basis of the ^1H NMR chemical shift of the analogous $[Fe(OEP)(CN)_2]^-$. The data in Table 4 indicate that $[Mn(TPP)(CN)_2]^-$ has much larger spin densities on the pyrrole carbons than $[Mn(T^iPrP)(CN)_2]^-$. The smaller spin densities on the pyrrole carbons in $[Mn(T^iPrP)(CN)_2]^-$ should be ascribed to the weak Mn (d_π) and porphyrin ($3e_g$) interactions due to the S_4 ruffling of the porphyrin ring. Since the d_{xy} orbital in $[Mn(T^iPrP)(CN)_2]^-$ is fully occupied by the electron pair, the deformation of the porphyrin core could not strengthen the Mn (d_{xy}) and porphyrin (a_{2u}) interaction in contrast to the case of the corresponding Fe(III) complex $[Fe(T^iPrP)(CN)_2]^-$.

Comparison with the Corresponding Fe(III) Complexes. We have recently reported that the electronic state of the low-spin iron(III) in $[Fe(Et\text{-}TPP)(CN)_2]^-$ is sensitively affected by the solvents used. For example, while the complex adopts the $(d_{xy})^2(d_{xz}, d_{yz})^3$ electron configuration in benzene, CCl_4, and acetonitrile, it exhibits the $(d_{xz}, d_{yz})^4(d_{xy})^1$ electron configuration in methanol, chloroform, and dichloromethane. Formation of the $(d_{xz}, d_{yz})^4(d_{xy})^1$ type complex in the latter solvents has been explained in terms of the intermolecular O−H···N or C−H···N hydrogen bonding between the solvent molecules and the coordinated cyanide ligands; the hydrogen bonding enhances the iron(d_π)−CN-(p_π*) interactions and stabilizes the $(d_{xz}, d_{yz})^4(d_{xy})^1$ electron configuration. Since the chemical shifts of the pyrrole protons and *meso* carbons correlate with the electron configuration of the low-spin iron(III) ion, we have concluded that the $(d_{xy})^2(d_{xz}, d_{yz})^3$ character increases as the solvent changes from CD_3OD to CCl_4 as shown in eq 15.[5]

$$CD_3OD < CDCl_3 < CD_2Cl_2 < (CD_3)_2CO, \text{DMSO-}d_6, \text{DMF-}d_7 < C_6D_6, C_6D_5CD_3, CD_3CN < CCl_4 \quad (15)$$

It should be noted that the order given in eq 15 parallels the order given in eq 3. Thus, while the intermolecular hydrogen bonding controls the electron configurations of low-spin iron(III) complexes $[Fe(Por)(CN)_2]^-$, it controls the product ratios [mono-adduct]/[bis-adduct] in the reaction between Mn(Por)-Cl and CN^-. Especially important is the fact that the product ratio changes to a great extent even between CH_2Cl_2 and $CHCl_3$; $Mn(T^iPrP)Cl$ (9.7 μM) is completely converted to the bis-adduct in CH_2Cl_2 solution though the conversion from the mono- to the bis-adduct is not observable even in the presence of 7000 equiv of $Bu_4N^+CN^-$ in $CHCl_3$ solution. The result clearly indicates that although $CHCl_3$ and CH_2Cl_2 are regarded as similar solvents in many aspects, they behave as completely different solvents especially in some coordination complexes.

Acknowledgment. This work was supported by the Fund for the Advancement of Science in commemoration of Toho University's 60th anniversary. A.I. thanks the Shibata Fund for Young Scientists in Toho University for financial support.

IC0206138